Exploiting of the Compression Methods for Reconstruction of the Antenna Far-Field Using Only Amplitude Near-Field Measurements

Jan PUSKELY, Zdeněk NOVÁČEK

Dept. of Radio Electronics, Brno University of Technology, Purkyňova 118, 612 00 Brno, Czech Republic

xpuske01@stud.feec.vutbr.cz, novacek@feec.vutbr.cz

Abstract. *The novel approach exploits the principle of the conventional two-plane amplitude measurements for the reconstruction of the unknown electric field distribution on the antenna aperture. The method combines a global optimization with a compression method. The global optimization method (GO) is used to minimize the functional, and the compression method is used to reduce the number of unknown variables. The algorithm employs the Real Coded Genetic Algorithm (RCGA) as the global optimization approach. The Discrete Cosine Transform (DCT) and the Discrete Wavelet Transform (DWT) are applied to reduce the number of unknown variables. Pros and cons of the methods are investigated and reported for the solution of the problem. In order to make the algorithm faster, exploitation of amplitudes from a single scanning plane is also discussed. First, the algorithm is used to obtain an initial estimate. Subsequently, the common Fourier iterative algorithm is used to reach global minima with sufficient accuracy. The method is examined measuring the dish antenna.*

Keywords

Planar near-field scanning, near-field far-field transform (NF-FF), global optimization, compression method, Fourier iterative algorithm.

1. Introduction

Conventional antenna radiation pattern measurements are performed in the far-field region which lies too far for electrically large antennas, and antenna test systems have to be fitted within actual test range of an anechoic chamber. In this case, far-field (FF) can be only determined by the measurement in the near field. The near-field measurement techniques are a powerful tool for characterizing antennas. Near-field (NF) measurements provide a fast and accurate method of determining the antenna gain, pattern, polarization, beam pointing etc.

Near-field to far-field (NF-FF) transformation techniques are based on the precision measurement. Complex-ity of setup and positioning system and its cost is increasing when dealing with electrically large antennas. In fact, obtaining the precise phase values of the electric field intensity is difficult at millimeter-wave and sub-millimeter-wave frequencies, unless expensive equipments are used. In order to overcome this problem, phaseless techniques which are able to evaluate the far-field pattern from the knowledge of near-field amplitude over one or more testing surfaces have been developed. Generally, two different approaches are used for solving the problem: interferometric and functional ones.

Interferometric methods employ Gabor holography and require a reference antenna for transmitting the phase reference to the receiving antenna. The reference signal interferes then with the signal transmitted by the antenna under test (AUT). The phase of the AUT signal is evaluated by a simple algorithm [1]. The interferometric method suffers some drawbacks, such as phase instability, and a requirement for accurate information about the pattern and position of the reference antenna.

On the contrary, functional techniques and the Fourier iterative method assume the knowledge of two sets of independent amplitude measurements [2]-[4]. These two sets can consist of the amplitudes on two separate planes, or the amplitudes measured by two different probes on the same plane.

All these approaches rely on the minimization of an amplitude-based functional. Minimization has to deal with the presence of local minima, due to the intrinsic non-convexity of the functional [2]. The minimization method can exploit local optimization techniques or global ones. In the case of local approaches, the effectiveness of the algorithm is conditioned by all available additional information of the AUT, by rough phase measurement in the near-field, or by using modified functional which reduces the occurrences of local minima. At the present, the functional minimization is mainly based on global optimization techniques which are very robust, when searching for the global minimum in a multidimensional domain [5], [6], [7]. On the other hand, this method requires large computational efforts.

In an attempt to use the benefits of interferometric

and functional methods, two probes were integrated together to take the measurement on the same plane and to mitigate the need for another antenna. This method requires an additional circuitry mechanism to add the probe voltages and their 90°-shifted values [8].

The method that utilizes phaseless electric field data over arbitrarily shaped surfaces for the reconstruction of an equivalent magnetic current density that represents the radiating structure of an antenna under test has been already published. The results were presented using phaseless data over one and two planes [9]. Accuracy of the results was better in case of using amplitude measurements over two surfaces, while the quality of the results using amplitude information on one scanning surface can strongly depend on the problem.

All these functional approaches suffer from a large numerical complexity or large computational efforts (in case of analysis of radiation properties of electrically large antennas, especially). The problem description comprises several thousands of unknowns, and CPU-time demands of the minimizing process are enormous. Hence, attention is turned to the representation of the unknown electric field distribution by few coefficients only.

In this paper, a novel method combining a global optimization with a compression method is presented. The method uses conventional two-plane amplitude measurements. The global optimization method (GO) is used to minimize the fitness function (functional) and the compression method (CoM) is used to reduce the number of unknown variables. The algorithm employs the Real Coded Genetic Algorithm (RCGA) as a global optimization tool [5]. Discrete Cosine Transform (DCT) and Discrete Wavelet Transform (DWT) are considered to reduce the number of unknown variables. Pros and cons of methods are investigated and reported for the solution of our problem. In order to make the algorithm faster, the exploitation of the amplitude from a single scanning plane only is discussed. So, this algorithm is used to obtain the initial estimation. Subsequently, the common Fourier iterative algorithm (FIA) is used to reach global minima with sufficient accuracy [6].

The RCGA/DCT (DWT) method exploited for the rough estimation of the global minima for a phase retrieval problem is presented in Section 2. Results obtained by applying the proposed algorithm are given in Section 3. The dish antenna has been measured in order to illustrate the applicability and accuracy of the proposed phase retrieval algorithm.

2. GO/CoM/FIA Method

The conventional minimization methods are based on the minimization of the difference between the calculated amplitudes and measured ones on two plane surfaces in the near-field region. Since we are looking for a rough estima-

tion only in the first part of the algorithm, we use the measured amplitudes from one scanning plane only and the comparison with two-plane algorithm is done. Thus, the process for obtaining the initial estimate is simplified and speeds up in the case of one-plane algorithm. The algorithm of the functional minimization assumes knowledge of the amplitudes on one (two) plane at least, scanning plane distance from the AUT and dimensions of the AUT (shown in Fig. 1).
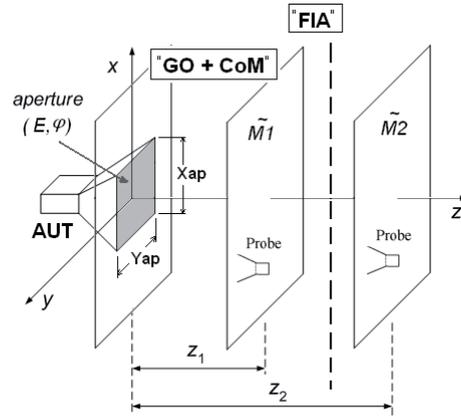

Fig. 1.   The principle of the minimization method.

Global optimization techniques are very useful in electromagnetic issues, when searching for a global maximum (minimum) in a multidimensional domain. In contrast to the local minimization, the use of the global algorithm is not conditioned by any choice of the initial estimation lying in the area of the global minimum and an additional modification of the minimized functional. On the other hand, minimizing process is not able to reach precise results and also convergence is relatively slow.

The presented algorithm (Fig. 2) excels in low computational requirements and simple implementation (the algorithm can be written in a few lines of a program code).

First, random initial estimate of the DCT (DWT) coefficients is performed. After the inverse DCT (DWT), we obtain electric field distribution on the antenna aperture. Zero padding is applied to the distribution to get the same extension as the scanning surfaces have. After this operation, the initial electric field on the aperture is transformed (using FFT) to the plane wave spectrum (PWS) and moved by the propagation constant to the distance of the first scanning plane and the second one. At this point, PWS at the first scanning surface and the second one are transformed back (using inverse FFT) to the electric field distribution (Fig. 2). In the next step, the computed amplitudes are compared with measured ones according to the preselected fitness function [10]. The fitness function is of the following form:

$$F = \sum_{i=1}^{N} \sum_{j=1}^{N} \left[\left| E_1(i,j) \right|^2 - \tilde{M}_1(i,j)^2 \right]^2 \cdot \tilde{M}_1(i,j) +$$
$$\sum_{i=1}^{N} \sum_{j=1}^{N} \left[\left| E_2(i,j) \right|^2 - \tilde{M}_2(i,j)^2 \right]^2 \cdot \tilde{M}_2(i,j) .$$

(1)

In (1), $E_1(i, j)$ and $E_2(i, j)$ are the computed complex electric field values in the point i, j on the first scanning surface and the second one, respectively. $\tilde{M}_1(i, j)$ and $\tilde{M}_2(i, j)$ are the measured amplitudes in the point i, j on the first scanning surface and the second one, respectively. The fitness function (1) represents an error that is subsequently minimized by the global optimization algorithm.
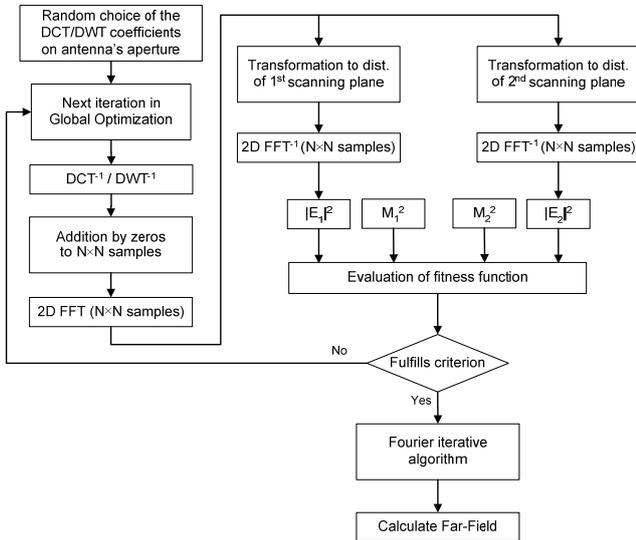

Fig. 2. The flow chart of the minimization algorithm exploiting a global optimization, a compression method and the Fourier iterative algorithm.

In next phase, the initial estimate is improved by the Fourier iterative algorithm which minimizes the same functional (1). For this purpose, we already use the measured amplitudes on both scanning planes to obtaining of the accurate results [9]. The success of the Fourier iterative algorithm as well as other local methods depends on achieving initial estimation which has to lie in a global minimum area [4].

2.1 Global Optimization: Real Coded Genetic Algorithms RCGA

Genetic algorithm is a stochastic method searching for a global minimum in a multidimensional domain. In analogy with the natural selection and evolution, the set of parameters to be optimized (genes) defines an individual (chromosome). The set of individuals forms the population, which is evolved by means of the selection, the crossover, and the mutation genetic operators (Fig. 3).

The number of chromosomes was set to 24 in the initial population. The tournament selection was the best selection strategy, and the linear crossover was the selected crossover strategy. For optimization, two strategies that are combined were designed, the crossing strategy and the mutation strategy [10]. In both cases, the probability of the crossover was set to $p_c = 100$ %, and the probability of the mutation to $p_m = 25$ %. The change in the strategy occurs when the convergence stagnates.
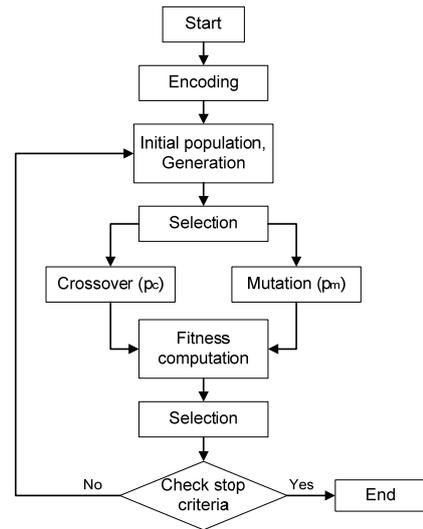

Fig. 3. Real coded genetic algorithm.

In Fig. 4, we can see the comparison of convergence properties for the two-plane minimization algorithm without DCT, for the two-plane minimization algorithm with DCT and for the one-plane minimization algorithm with DCT. In each case, the functional (1) was minimized. Ten repeats were performed and the optimization was stopped in the 2000th iteration. The convergence properties were investigated for the dish antenna (section 3).
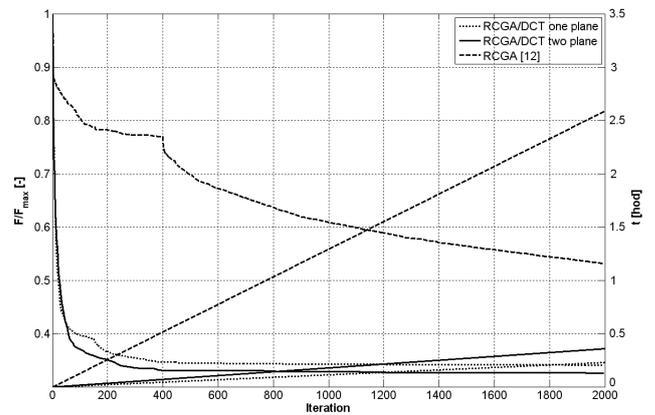

Fig. 4. Comparison of convergence properties for two-plane algorithm without DCT, two-plane algorithm with DCT and one-plane algorithm with DCT.

Obviously, the algorithm using DCT exhibits better convergence properties. Although the implementation of the compression method is quite time-consuming operation the algorithm brings remarkable optimization time savings. It is because only a fraction of the coefficients (50 coefficients) representing searched electric field on antenna aperture was optimized (Fig. 4). The number of used planes has only a small effect on the convergence properties of the algorithm.

2.2 Compression Methods: DCT and DWT

Two compression methods were applied in order to reduce the number of unknowns – the 2D discrete cosine

transform and the 2D discrete wavelet transform. The verification of properties of both the methods was carried out by the radiation pattern reconstruction of the 60-mm Teflon lens antenna, which was analyzed at 310 GHz [11]. The measurements of the lens antenna for the analysis in [11] were carried out at Aalto University School of Science and Technology, Finland (formerly TKK Helsinki University of Technology). The lens antenna and the measurement setup are briefly described in [12].

2.2.1 Discrete Cosine Transform DCT

In 1974, the discrete cosine transform (DCT) was introduced by Ahmed, Natarajan, and Rao [13]. In particular, the DCT was categorized into four slightly different transformations named DCT-I, DCT-II, DCT-III, and DCT-IV. The DCT-II is concerned in this paper. The DCT is often used in signal and image processing, for lossy data compression especially. The DCT converts data into sets of frequencies. The first frequencies in the set are the most significant, and the latter frequencies are of lower significance. In order to compress data, the least significant frequencies are neglected based on an allowable resolution loss. The definition of the 2D DCT-II for an input data A and output data B is

$$B_{pq} = \alpha_p \alpha_q \sum_{p=0}^{M-1}\sum_{q=0}^{N-1} A_{mn} \cos\frac{\pi(2m+1)p}{2M} \cos\frac{\pi(2n+1)q}{2N} \quad (2a)$$

$$\alpha_p = \begin{cases} 1/\sqrt{M}, & p = 0 \\ \sqrt{2/M}, & 1 \le p \le M\text{-}1 \end{cases} \quad (2b)$$

$$\alpha_q = \begin{cases} 1/\sqrt{N}, & q = 0 \\ \sqrt{2/N}, & 1 \le q \le N\text{-}1 \end{cases} \quad (2c)$$

where M and N denote the number of rows and columns of $\mathbf{A}$, respectively. The inverse transform is defined:

$$A_{mn} = \sum_{p=0}^{M-1}\sum_{q=0}^{N-1} \alpha_p \alpha_q B_{pq} \cos\frac{\pi(2m+1)p}{2M} \cos\frac{\pi(2n+1)q}{2N} . \quad (3)$$

The influence of the number of coefficients which are used for the reconstruction of the unknown field distribution and its error is analyzed. The analyses are performed using the electric field intensity of a lens antenna, a dish antenna and an antenna array (27×13 elements). In Fig. 5, the dependence of the calculated error on the number of coefficients, which are taken into account for the reconstruction of the fields, are depicted. Obviously, we are not able to generalize the dependence of the error on the number of coefficients accurately. If precise results are required, more than 20 % of coefficients (the blue area) have to be taken into account. If a rough estimate is needed, less than 0.5 % of coefficients (the grey area) have to be considered.

For the lens antenna, the analysis of the dependence of the error of the field distribution on the number of coefficients was performed. We took into account three different numbers of coefficients (Fig. 5): P1 = 19 coefficients (0.1% of all coefficients), P2 = 397 coefficients (2%),

P3 = 4373 coefficients (22%). Then, we made the inverse discrete cosine transform IDCT and calculated the radiation patterns (Fig. 6).
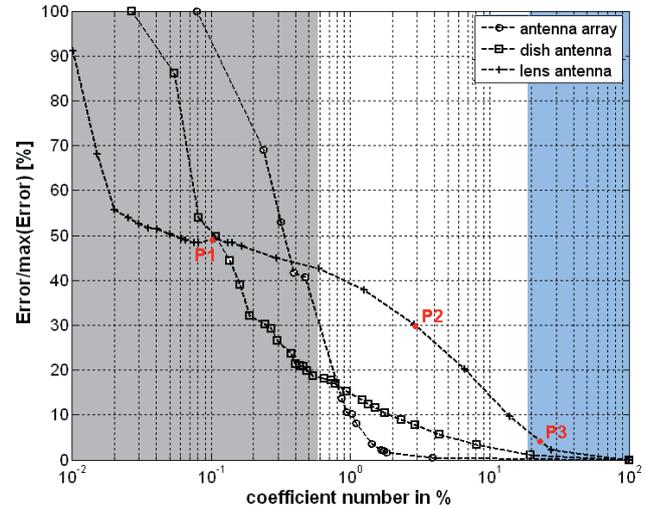

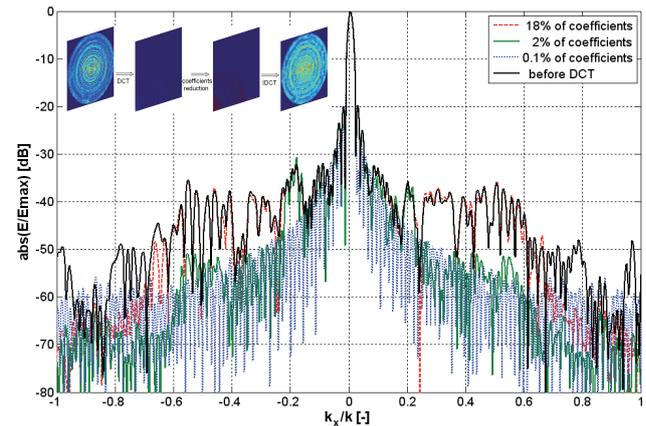**Fig. 5.** Dependences of the calculated error on the number of coefficients.

Fig. 6. Top: principle of the analysis. Bottom: calculated radiation patterns of the lens antenna for the different number of coefficients.

As obvious from Fig. 6, high frequency terms relate to the far-side lobes, which are at lower level and therefore are not taken into account. 18% of the coefficients relates to $k_x/k \le \pm0.6$ and 2% of the coefficients to $k_x/k \le \pm0.2$. It follows that a large number of coefficients ensures a good agreement between the required pattern and the reconstructed one. On the other hand, if a fraction of variables is used, a rough estimate of the radiation pattern is obtained, and the agreement is achieved in the domain of the main lobe only.

In Fig. 7, the influence of the coefficient error is depicted. Coefficients were loaded by a random error up to 30% from the maximum value of the coefficient. Clearly, the calculated mean square error from the reconstructed electric field distribution grows exponentially with the error of the coefficient. Obviously, the error dependence is stronger for the increasing number of coefficients. When

optimizing a very large number of the coefficients starting from a random initial guess, the finding of the solution can be very lengthy.
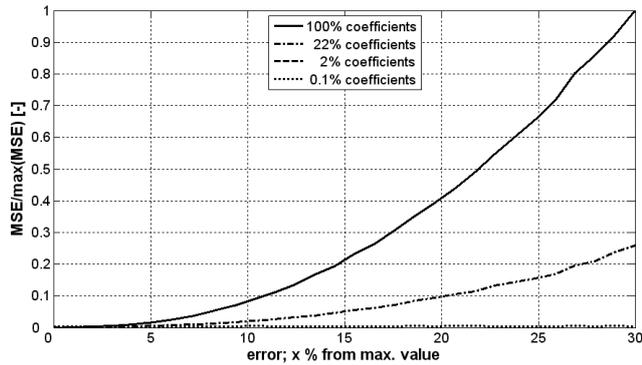

Fig. 7. The influence of the coefficient error.

In case of DCT, precise results require a large number of coefficients. But, a very strong influence of errors is a disadvantage. We therefore have to use an initial estimate calculated from the electric field distribution on the first scanning plane. If only a rough estimate is needed, a random guess of a fraction of coefficients can be used. For that reasons, the compromise between these two cases is better to be chosen.

2.2.2 Discrete Wavelet Transform DWT

The discrete wavelet transforms are based on the recurrence relations to generate progressively finer discrete samplings of an implicit mother wavelet function [14]. The discrete wavelet transform has a huge number of applications in science.

The DWT analyzes the signal in different frequency bands with different resolutions by decomposing the signal into a coarse approximation and detail information. The DWT employs wavelet functions, which are associated with low pass and high pass filters, respectively. For images, two-dimensional wavelets are exploited. The resulting 2D array of coefficients contains four bands of data, the approximation CA, and the details in three orientations (horizontal $CD^{(h)}$, vertical $CD^{(v)}$, and diagonal $CD^{(d)}$), corresponding to the first level of the image decomposition. The CA band can be further decomposed in the same manner for the second level of the decomposition. This can be done up to any level, thereby resulting in a pyramidal decomposition. Two-level decomposed image is depicted in Fig. 8b and the filter bank structure of the 2D-DWT decomposition is shown in Fig. 8a. Bi-orthogonal wavelets were used as decomposition and reconstruction filters in this case.

In the case of DWT, the influence of the number of the decomposition steps and the influence of random errors is analyzed. Analyses were also performed for the lens antenna.

The influence of the decomposition steps is shown in Fig. 9. Each decomposition leads to a fourfold reduction of

variables. After three decompositions, the number of unknowns is reduced 64 times. For three decomposition steps, the electric field distribution and calculated radiation patterns are depicted in Fig. 9. Fig. 9 shows the agreement in domain $|k_x/k| = 0.15$ for all decompositions but the agreement in a wide range can be observed in case of a single decomposition step only.
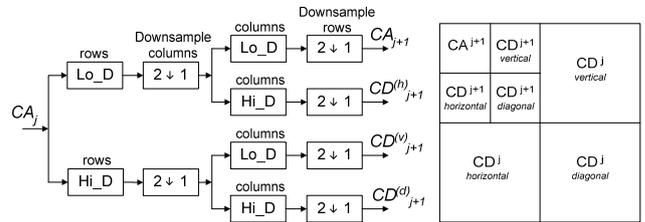

Fig. 8. Image decomposition using DWT; left: filter bank structure for one level of image decomposition; right: two level scheme.
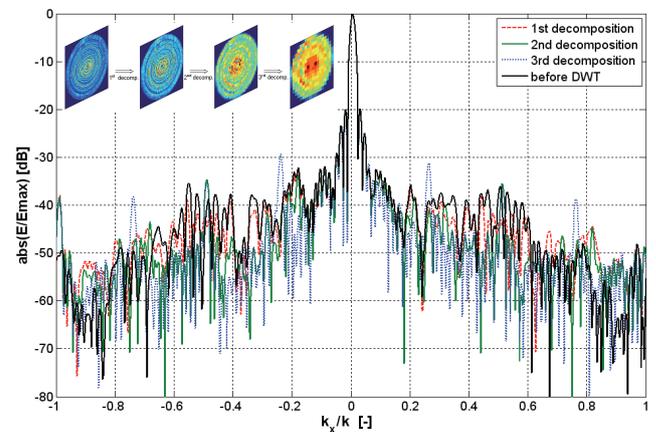

Fig. 9. Top: Electric field distributions obtained by decompositions; Bottom: Calculated radiation patterns of the lens antenna for different number of the decompositions.

In Fig. 10, the effect of the random error in the decomposed electric field distribution is analyzed. Clearly, the error in the reconstructed electric field distribution grows exponentially with the increasing random error. The error effect is more significant in cases, when a larger number of unknowns is optimized. Further, the DWT is less sensitive to the random error than DCT, and the random initial guess can be always used.
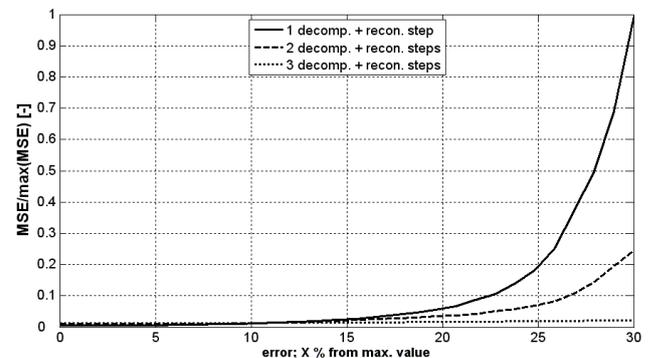

Fig. 10. Analyses of the influence of the random error.

Dealing with DWT, only one decomposition step (fourfold reduction) can be considered to obtain accurate results, but the influence of errors is very significant then. Therefore, we are looking for estimation only. Using more than a single decomposition is more useful.

Shortly, DCT and DWT are easy to implement. The reduction of the number of optimized variables is in favor of DCT. If more than rough estimates are required, the initial estimate calculated from the electric field distribution on the first scanning plane should be used. Since DWT is less sensitive to the random error than DCT, the initial guess can be chosen randomly.

3. Experimental Results

The verification of the described novel method was carried out on the radiation pattern reconstruction of the dish antenna [6].
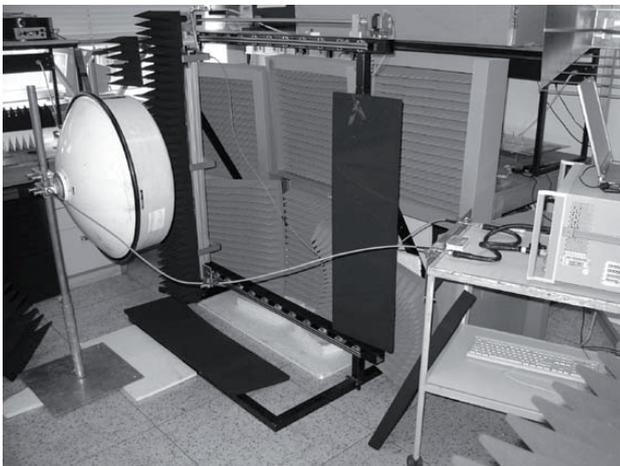

Fig. 11. The measurement site arrangement.

The dish antenna with the reflector diameter of 0.6 m was analyzed. The measurement site is shown in Fig. 11. As the scanning probe, the waveguide R140 was used. The values of the horizontal electric field intensity component in discrete points placed in the vertical direction and the horizontal one with the pitch of 10 mm (0.48λ) at two scanning planes of the size 800×800 mm were measured by a probe. Generally, 6 551 (81×81) values on each plane were achieved. The first plane was placed in the distance of 268 mm (~12.86λ), and the second one in the distance of 298 mm (~14.3λ). These distances correspond to the valid angle $\theta_v = 18.55^o (|k_x/k| = |k_y/k| = 0.32)$. Since the aperture of the antenna is 600×600 mm (61 times 61 sampling points), the solution space contains 3 721 complex parameters whose optimal values are going to be found out.

The contour plot of the near-field directly measured by the probe at frequency 14.4 GHz is depicted in Fig. 12 and 13 for both the amplitude and the phase.

The both compression methods were used for the initial reconstruction of the phases and amplitudes on the

antenna aperture. The far-field results obtained by the methods RCGA/DCT and RCGA/DWR are shown in Fig. 14 and 15 respectively. Fig. 14 shows the reconstructed radiation pattern which was achieved by the RCGA/DCT. For the reconstruction, approximately 6% of all the coefficients were used.
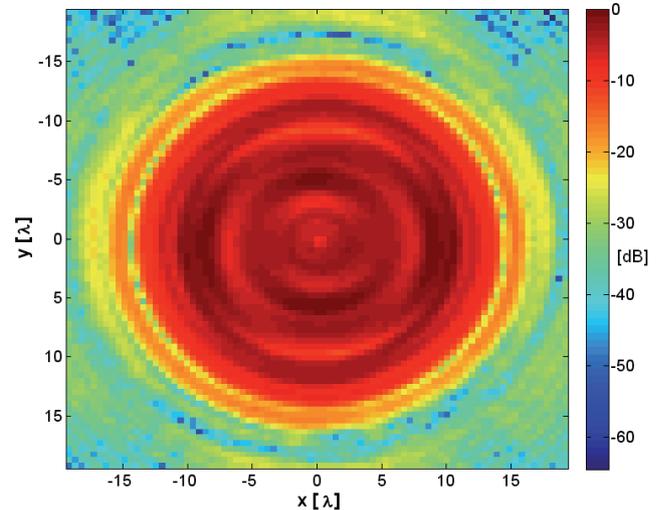

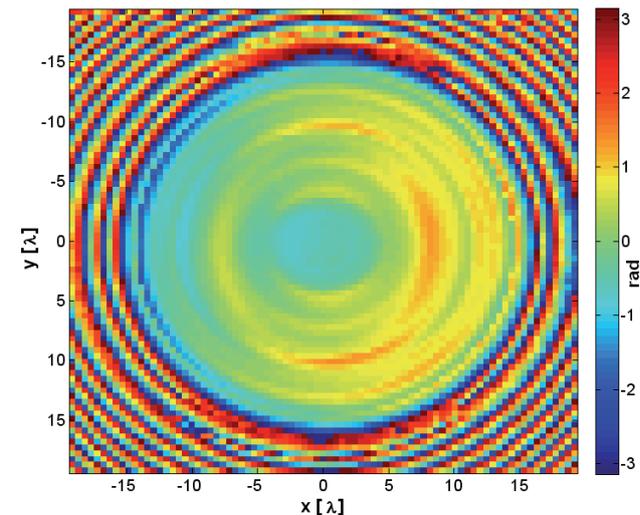**Fig. 12.** Near-field amplitude on the 2nd scanning plane.

Fig. 13. Near-field phase on the 2nd scanning plane.

The radiation pattern obtained after applying the RCGA/DWT is shown in Fig. 15. In the case of DWT, two decompositions (16 times reduction) were used. The reconstructed far-field radiation patterns prove that we can use only amplitude on one plane for achieving the initial estimate. After this, we applied the Fourier iterative algorithm and exploited the knowledge of amplitudes on both scanning planes to ensure the required precision of the radiation patterns.

The agreement of retrieved near-field phase and the exact one is shown in Fig. 16. The phase distributions reported in Fig. 13 and Fig. 16 show that obtained retrieved phase distribution is in good match with the measured one in the central zone of the radiated field.
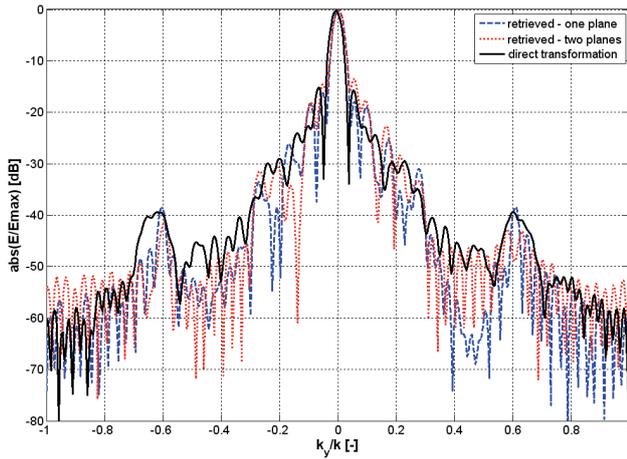
Fig. 14. Reconstructed E plane radiation pattern of the dish antenna after applying RCGA/DCT.
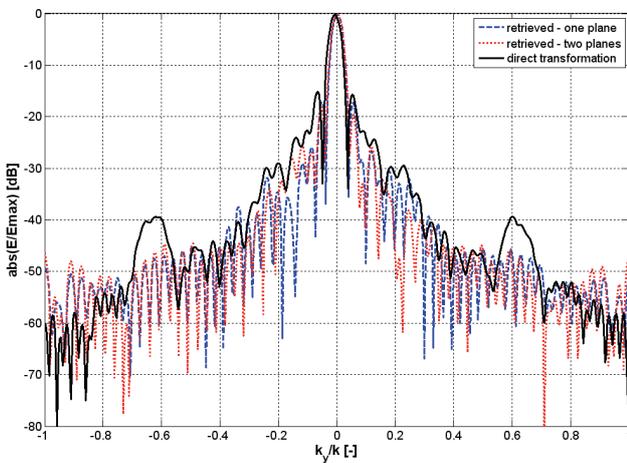

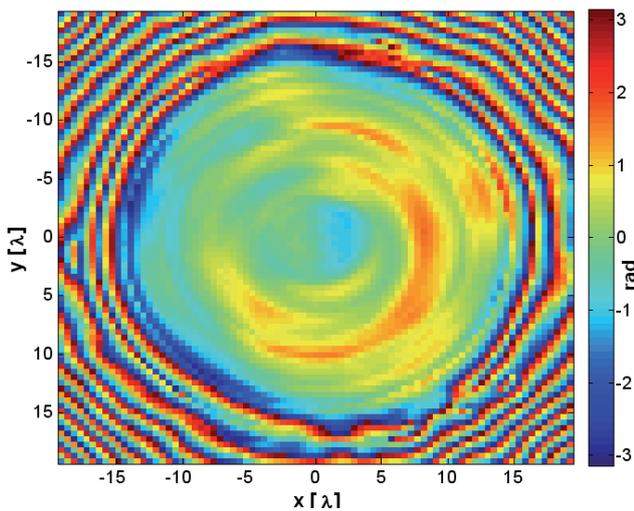**Fig. 15.** Reconstructed E plane radiation pattern of the dish antenna after applying RCGA/DWT.

Fig. 16. Retrieved near-field phase on the 2nd scanning plane.

The far-field results obtained by the method RCGA/DCT and the FIA are shown in Fig. 17. The agreement between the far-field obtained from the retrieved and directly measured near-field amplitude and phase is excellent. The algorithm was used at frequency 12.3 GHz also.

The obtained radiation pattern of the dish antenna is shown and successfully compared with the result provided by direct near-field amplitude and phase measurements in Fig. 18.
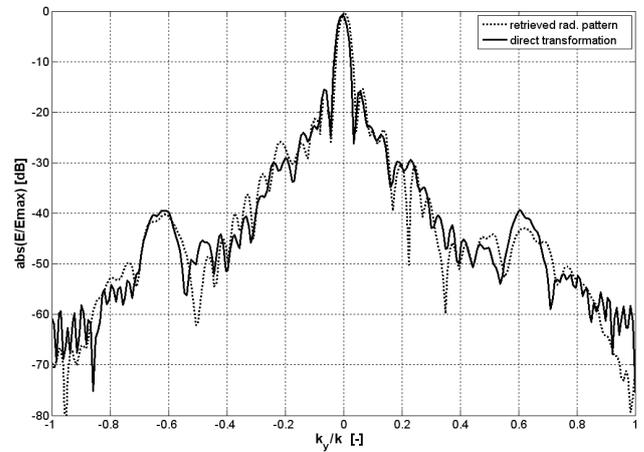

Fig. 17. Comparison between the far-field obtained from the accurate and retrieved near-field phase (E plane) at f = 14.4 GHz.
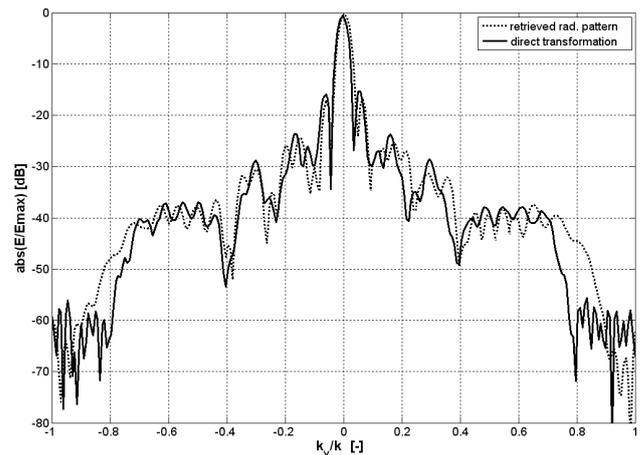

Fig. 18. Comparison between the far-field obtained from the accurate and retrieved near-field phase (E plane) at f = 12.3 GHz.

4. Conclusions

A novel near-field phaseless approach for the antenna far-field characterization is presented in this paper. The method combines a global optimization, a compression method and a Fourier iterative algorithm in conjunction with conventional two-plane amplitude measurements.

The global optimization method (RCGA) is used to minimize the functional, the compression method (DCT) is used to reduce the number of unknown variables, and the Fourier iterative algorithm is used to improve the estimate achieved by RCGA/DCT.

Amplitude-only data over a single plane were used to obtain the initial field distribution estimate. If rough estimate of field distribution is required only, the amplitude

from a single plane can be considered only. For obtaining precise results, two sets of amplitudes are necessary.

The proposed algorithm is very robust and faster than comparable algorithms available. The algorithm does not require any initial guess in the region of the global minima and any additional information about the AUT. The application of the described algorithm for the phase reconstruction of the dish antenna was presented. The far-field patterns from the phase retrieval algorithm were shown to have a very good agreement with the results of complex near-field measurements (amplitude and phase).

Acknowledgements

References

[1] JUNKIN, G., BENNET, J. C., HUANG, T. Holographic near-field /far-field for therahertz antenna testing. In *Proceedings of 19th Antenna Measurement Tech. Assoc. Meet. Symposium.* Boston (USA, MA), Nov. 1997, p. 419 - 423.

[2] BUCCI, O. M., D'ELIA, G., LEONE, G., PIERRI, R. Far-field pattern determination from the near-field amplitude on two surfaces. *IEEE Transaction on Antennas and Propagation*, 1990, vol. 38, no. 11, p. 1772 - 1779.

[3] PIERRI, R., D'ELIA, G., SOLDOVIERI, F. A two probes scanning phaseless near-field far-field transformation technique. *IEEE Transaction on Antennas and Propagation*, 1999, vol. 47, no. 5, p. 792 - 802.

[4] YACCARINO, R. G., RAHMAT-SAMII, Y. Phaseless bi-polar planar near-field measurements and diagnostics of array antennas. *IEEE Transactions on Antennas and Propagation*, 1999, vol. 47, no. 3, p. 574 – 583.

[5] PUSKELY, J., NOVÁČEK, Z. Application of the global optimization approaches to planar near-field antenna phaseless measurements. *Radioengineering*, 2009, vol. 18, no. 1, p. 9 - 17.

[6] TKADLEC, R., NOVÁČEK, Z. Radiation pattern reconstruction from the near-field amplitude measurement on two planes using PSO. *Radioengineering*, 2005, vol. 14, no. 4, p. 63 - 67.

[7] RAZAVI, S. F., RAHMAT-SAMII, Y. A new look at phaseless planar near-field measurements: limitations, simulations, measurements, and a hybrid solution. *IEEE Antennas and Propagation Magazine*, 2007, vol. 49, no. 2, p. 170 - 178.

[8] COSTANZO, S., DI MASSA, G., MIGLIORE, M. D. A novel hybrid approach for far-field characterization from near-field amplitude-only measurements on arbitrary scanning surfaces. *IEEE Transactions on Antennas and Propagation*, 2005, vol. 53, no. 6, p. 1866 - 1874.

[9] LAS-HERAS, F., SARKAR, T.-K. A direct optimization approach for source reconstruction and NF-FF transformation using amplitude-only data. *IEEE Transactions on Antennas and Propagation*, 2002, vol. 50, no. 4, p. 500 - 510.

[10] PUSKELY, J., NOVÁČEK, Z. New look to Real Valued Genetic Algorithm used to reconstruct radiation patterns. In *Proceedings of the 15th Conference Radioelektronika 2009*. Bratislava (Slovakia), 2009, p. 299 - 302.

[11] PUSKELY, J., NOVÁČEK, Z. Reconstruction of antenna radiation pattern at 310 GHz using image compression methods. In *Proceedings of the 4th European Conference on Antennas and Propagation EuCAP 2010*, 2010.

[12] VON LERBER, A., VIIKARI, V., LISENO, A., ALA-LAURINAHO, J., RÄISÄNEN, A. V. A feasibility study of phase retrieval algorithms at sub-millimeter wavelengths. In *Proceedigns of the 27th Annual Antenna Measurement Techniques Association (AMTA) Meeting & Symposium*. Newport (RI, USA), 2005, p. 79 to 84.

[13] AHMED, N., NATARAJAN, T., RAO, K. R. Discrete cosine transform. *IEEE Transactions Computer*, 1974, vol. COM-23, no. 1, p. 90 - 93.

[14] DAUBECHIES, L. The wavelet transforms, time-frequency localization and signal analysis. *IEEE Transactions on Information Theory*, 1990, vol. 36, no. 5, p. 961 - 1005.

About Authors...

Jan PUSKELY was born in Přerov, Czech Republic, in 1982. He received his master's degree in electrical engineering from the Brno University of Technology in 2007. At present, he is a PhD student at the Department of Radio Electronics, Brno University of Technology. His research interest is focused on measurements in the near field of antennas.

Zdeněk NOVÁČEK was born in 1945 in Kamenná, Czech Republic. He received his master's degree in 1969 and CSc. (PhD) degree in 1980, both from the Brno University of Technology. Since 1969, he worked as Senior lecturer and since 1997 as Associated Professor at the Department of Radio Electronics, Brno University of Technology. His research interests are focused on the theory of electromagnetic field, antennas and propagation of radio waves, mobile antennas, antenna measurements and the space-time signal processing.